

To be presented at the IEEE Industry Applications  
Society 1984 Annual Meeting, Chicago, IL,  
September 30 - October 4, 1984

DEVELOPMENT OF NOVEL LAMPS FOR STUDY OF ENHANCED  
PRODUCTION OF RESONANCE RADIATION BY  
LOW-DENSITY MERCURY DISCHARGES

Z.-X. Wang, D.D. Hollister, and S.M. Berman

June 1984

DEVELOPMENT OF NOVEL LAMPS FOR STUDY  
OF ENHANCED PRODUCTION OF RESONANCE  
RADIATION BY LOW-DENSITY MERCURY DISCHARGES

Z.-X. Wang,\* D.D. Hollister, and S.M. Berman

Lighting Systems Research  
Lawrence Berkeley Laboratory  
University of California  
Berkeley, CA 94720 U.S.A.

**Abstract**—A novel mercury-argon discharge tube is described. It incorporates two identical condensation pump “cold spots” that are employed to determine both the mercury sorption rate and the coefficient of free diffusion for mercury in argon. Equilibration periods for this system are found to depend in part on the temperature difference between the two cold-spot surfaces, and on the separation of these surfaces. Sorption of mercury at the discharge tube’s surface, and the subsequent cleanup of the mercury charge, is determined by the time rate of change of the equilibration period.

Data accumulated during these tests are incorporated into the design scheme of discharge tubes intended for Zeeman-effect and isotope blending studies described elsewhere.

### I. Introduction

In studying the effects of isotope blending [1,2] on the production efficiency of resonance radiation by a low-density mercury discharge, it became necessary to evaluate, for several glasses, the rate of depletion of natural mercury from the discharge tube in order to anticipate the proper time to admit to the discharge precise quantities of a specific mercury isotope. The principal mechanism of mercury depletion is absorption by the discharge tube glass, and this has been treated recently by van Heusden and Mulder [3–5] who observed that, following an initial rapid penetration into the surface of the glass, a much slower migration process enables the penetration by mercury to a depth of about 30 nm. This leads to an agglomeration of mercury inside the glass, eventually forming metallic mercury droplets, and therefore reducing the effective mercury content of the discharge tube.

For purposes of the experiment it was necessary to determine the extent of mercury depletion as a function of discharge tube operating time. By designing a highly efficient condensation pump and mounting one of these behind each electrode, a discharge tube was developed that is capable of determining the depletion rate of its mercury charge. The salient features of this design are described below.

### II. Considerations of Cold-Spot Design

In a mercury vapor discharge tube, the partial pressure of mercury is usually determined by the temperature of the coldest part of the discharge tube. This location is aptly called the tube’s “cold spot.”

In reality the cold spot is a condensation pump operating between ambient temperature  $T$  where the partial pressure of the vapor is  $P_1$ , and the cold-spot temperature  $T_c$ , where the pressure of the vapor is  $P_2$ . The rates at which particles arrive at and depart from the cold spot are determined from kinetic theory, and their difference is the rate of particle depletion from the discharge tube volume:

$$\frac{dn}{dt} = P_1 N_0 A (2\pi MRT)^{-1/2} \left( 1 - \frac{P_2}{P_1} \right) \text{ particles/second} \quad (1)$$

The effective pumping speed is then

$$S = A(RT/2\pi M)^{1/2} \left( 1 - \frac{P_2}{P_1} \right) \text{ cc/sec} \quad (2)$$

where  $N_0$  is Avogadro’s number,  $6.025 \times 10^{23} \text{ mol}^{-1}$ ;  $R$  is the universal gas constant,  $8.317 \times 10^7 \text{ erg/}^\circ\text{C mol}$ ;  $A$  is the effective area of the cold spot;  $M$  is the molecular weight of the condensable vapor; and  $T$  is the ambient temperature.

For the cold spot to be effective in controlling the condensable vapor pressure, the area  $A$  should be large and the vapor pressure of the condensed vapor at the cold spot  $P_2$  should be much less than  $P_1$ , the partial pressure of the vapor in the system. The ultimate pressure will be  $P_2$ . If the cold-spot is connected to the discharge tube through a conductance that is small compared to the pumping speed, the conductance determines the effective cold-spot pumping speed. If the conductance is large, the pumping speed is limited only by the pump itself [6]. For example, the conductance of a circular pipe is proportional to the cube of its diameter and inversely proportional to its length, so it would be appropriate to connect the cold-spot condensation pump to the discharge tube through a very short pipe with a large diameter.

The location of the cold spot is also of importance in terms of discharge tube operation. In the positive columns of discharges of interest here the electrical conductivity  $\sigma$  is a scalar quantity and Ohm’s law is given by  $\vec{j} = \sigma \vec{E}$ . Taking the divergence of both sides of this expression gives

$$\nabla \cdot \vec{j} = \vec{\nabla} \sigma \cdot \vec{E} + \sigma (\nabla \cdot \vec{E}) \quad (3)$$

The first term vanishes by charge conservation and the last term vanishes because of charge neutrality. Noting that  $\sigma = \sigma(T)$ ,  $\nabla \sigma = \nabla \sigma(T) = (d\sigma/dT) \nabla T$ , and the middle term of Eq. (3) leads to

$$\vec{E} \cdot \vec{\nabla} T = 0 \quad (4)$$

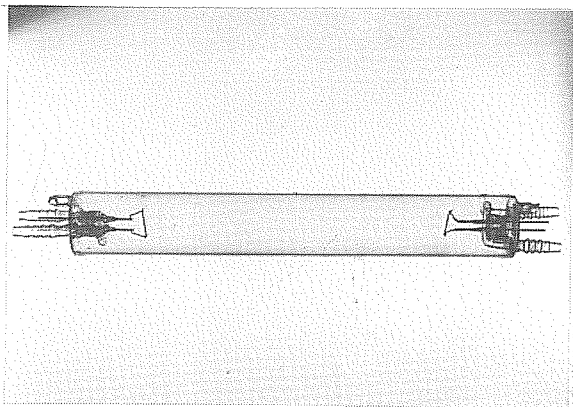
Thus, in the positive column of the metal-vapor discharge, the equipotentials and isotherms are orthogonal and the current flows on the isothermal surfaces [7]. Evidently, location of the cold spot in the vicinity of the positive column may affect the discharge by modifying the temperature gradient in Eq. (4). The cold spot therefore must not be directly adjacent to the arc. This, coupled with the earlier consideration of the need for a high-conductance path between the cold spot and the positive column, led to the conclusion that the only viable location for the cold spot in the discharge tube is within the tube itself, behind the filament.

The initial cold-spot design was a 2-1/2 turn coil of borosilicate glass mounted behind a filament. Water, circulated through this coil, determined the cold-spot temperature, which was conveniently monitored with an in-line thermistor. It was initially feared that, because the cold spot faced the arc on only one side, its effective area may be reduced considerably and, from Eq. (2), the condensation pump’s pumping speed would be low. This was not found to be the case and, in the next iteration of this design, the difficult-to-assemble glass coil was effectively replaced by a simple, single length of glass tubing at the same location.

In earlier work [2] discharge tubes were fabricated in four-foot lengths to enable the direct comparison of discharge electrical and

\*Permanent address: Institute of Electric Light Sources, Fudan University, Shanghai, China.

radiation measurements with similar observations from standard fluorescent lamps. To combat the cleanup and subsequent disappearance of mercury isotope blends in the original experimental discharge tubes, envelope surface areas were substantially reduced by shortening the length of the tubes to 25.4 cm. The diameter remained fixed at 3.8 cm. These dimensions were retained. A photograph of the final form of the discharge tube appears in Fig. 1.



CBB 845-3956

Fig. 1. Photograph of experimental discharge tube showing electrode structures and dual condensation "cold-spot" pumps.

### III. The Diffusion Mechanism

The experimental discharge tube shown in Fig. 1 contains two condensation pumps, and was designed to enable the measurement of sorption of mercury by its glass walls. In operation, one condensation pump is cooled to a temperature in the vicinity of 1°C while hot water is pumped through the other condensation pump, and

the remainder of the discharge tube is maintained at a much higher temperature. After a brief equilibration time, most of the tube's charge of mercury will condense on the cold spot, and, as a result, the radiant output of the discharge tube is significantly reduced. It is said that the cold spot is then "in control" of the mercury vapor pressure. Next, the roles of the two condensation pumps are suddenly reversed by simultaneously switching the cold water flow to the hot condensation pump and the hot water flow to the original cold spot. The lamp's charge of mercury now must evaporate from the hot surface (i.e., surface 1) and diffuse through the length of the lamp to condense on the new cold spot (surface 2). Since the condensation pumps' temperatures are held constant, the rates of evaporation and condensation of mercury vapor are fixed, and a steady state is quickly established in which the rate of mercury transport from surface 1 to the cold spot at surface 2 is constant. This steady diffusion will continue through a period  $\tau$  until nearly all of the mercury from surface 1 condenses on surface 2. Figure 2 shows the mercury concentration gradient along the length of the discharge tube during this period. At the end of this period the mercury vapor pressure will decrease at a rate determined by the pumping speed of surface 2 until the mercury concentration everywhere in the discharge tube is determined by the vapor pressure above surface 2.

The total quantity  $Q$  of mercury transported from surface 1 to surface 2 during the period  $\tau$  is given by  $-JS_c\tau$ , where  $J$  is the diffusion current density and  $S_c$  is the cross section of the discharge tube. If the mercury concentration gradient is  $dn/dx$ , the transported quantity becomes

$$Q = -DS_c\tau \frac{n_2 - n_1}{\ell}, \quad (5)$$

where  $D = J(dn/dx)^{-1}$  is the coefficient of free diffusion for mercury in argon at the filling pressure of 3 torr;  $n_1$  and  $n_2$  are the equilibrium concentrations of mercury above surfaces 1 and 2, respectively; and  $\ell$  is the distance between the two surfaces. The period  $\tau$  depends only on the amount of mercury within the lamp if the temperatures at surfaces 1 and 2 are kept constant:

$$\tau = Q/DS_c \frac{n_1 - n_2}{\ell}. \quad (6)$$

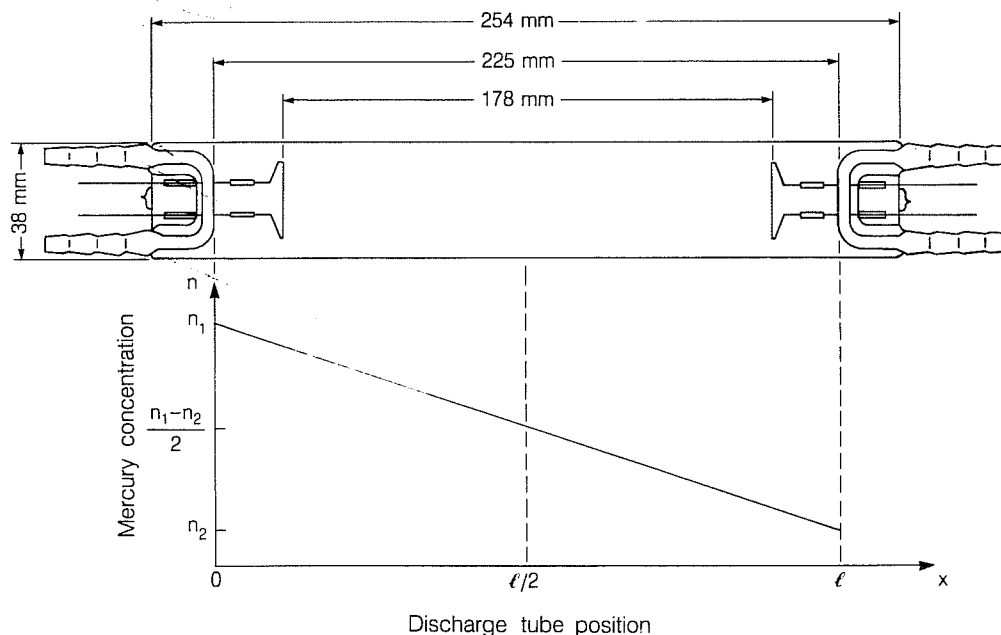


Fig. 2. Side view of discharge tube showing mercury vapor concentration distribution along the length of the discharge tube.

Thus, if the discharge tube envelope sorbs mercury, the quantity  $Q$  of mercury that diffuses within the tube will diminish, and this will result in a decrease in  $\tau$ .

Sorption of mercury by the envelope is relatively slow, and the envelope does not rapidly become saturated with mercury. The effects of desorption therefore are not expected to be significant during diffusion time measurements, and are neglected. Then, the amount  $dq$  of mercury sorbed in the time  $dt$  is

$$dq = -knS_s dt \quad (7)$$

where  $n$  is the mercury concentration, a function of the cold-spot temperature,  $S_s$  is the inner surface area of the discharge tube, and  $k$  is the sorption rate per unit of envelope area which, except during the initial several-to several-tens of operating hours [5], is essentially constant. If this non-constant period is sufficiently short, its nonlinear contribution will be negligibly small in the integral of Eq. (7), namely

$$q = -knS_s t \quad (8)$$

Initially the mercury content of the discharge tube is  $Q_0$  and the sorbed quantity is  $q_0 = 0$ . At an accumulated time of operation  $t_1$  the sorbed mercury is  $q_1 = -knS_s t_1$ , and the unsorbed mercury is

$$Q_1 = -D \frac{n_2 - n_1}{\ell} S_c \tau_1 \quad (9)$$

where

$$q_1 = Q_1 - Q_0 \quad (9)$$

Then, by substitution,

$$-knS_s t_1 = -D \frac{n_2 - n_1}{\ell} S_c \tau_1 - Q_0 \quad (10)$$

and, at the accumulated time  $t_2$ ,

$$-knS_s t_2 = -D \frac{n_2 - n_1}{\ell} S_c \tau_2 - Q_0 \quad (11)$$

Combining of Eqs. (10) and (11) yields two equations in two unknowns:

$$D = \frac{Q_0}{S_c} \left/ \left( \frac{n_1 - n_2}{\ell} \right) \cdot \left\{ \left( \frac{\tau_1 - \tau_2}{t_2 - t_1} \right) t_1 + \tau_1 \right\} \right. \quad (12)$$

and

$$k = \frac{DS_c}{nS_s} \left( \frac{n_1 - n_2}{\ell} \right) \left( \frac{\tau_1 - \tau_2}{t_2 - t_1} \right) \quad (13)$$

#### IV. Experimental Techniques

Three nearly identical discharge tubes were fabricated of borosilicate, lead, and quartz glass, respectively. Two of these were provided with central quartz windows to facilitate viewing 254 nm radiation, and all were charged with about 9 mg of natural mercury and backfilled with argon to a pressure of 3.0 torr. Each was equipped with two condensation pumps, as previously described. One such pump, which served as the discharge tube's cold spot, was supplied water at a temperature of 1°C from an ice bath. The other condensation pump was held at 56°C by means of an SCR proportional temperature controller. Constant ambient conditions were maintained by mounting the discharge tube in a heated box through which a gentle flow of argon was bled. The tube's wall temperature was about 75°C.

The 254-nm resonance radiation emitted in the central plane of the discharge tube was detected by a vacuum photodiode that viewed the discharge through a slit and a narrow-band filter with

transmission centered at 254 nm. The output signal was amplified and displayed as a function of time on a strip-chart recorder. Also displayed were a voltage proportional to the resistance of a thermistor mounted in the cold-spot water flow line, and the voltage across the discharge tube. Current through the discharge tube was held constant at 400 ma.

With the cold spot in control of the mercury vapor pressure and all other parameters held fixed, a typical diffusion time measurement would begin when the roles of the cold and hot spots were suddenly reversed by switching water supplies. At this moment the mercury vapor pressure would rise to a level determined by the hot-spot temperature, the new cold spot would begin its mercury condensation cycle, and the photodiode output would suddenly rise in response to the increase in mercury vapor pressure. In general, with the given temperatures, it would take the new cold spot about 1 hour to condense all the mercury evaporated by the hot spot; that is, to take control of the vapor pressure. At this time, the photodiode output would exponentially decrease at a rate determined by the cold spot's pumping speed.

Figure 3 shows a drawing of a typical diffusion time record, in which are displayed three traces: trace 1 is the photodiode output, trace 2 is the voltage across the discharge tube, and trace 3 is the output of the thermistor located in the original cold-spot water line. It is a characteristic of the recording instrument that trace 3 and trace 1 are offset by plus and minus one-half division, respectively, from trace 2. The sweep rate was 1/2 division per minute.

The slight overshoot of the beginning of the photodiode output trace indicates the onset of severe self-absorption of resonance radiation by the discharge. The emission peak occurs at a concentration of roughly  $2.9 \times 10^{14} \text{ cm}^{-3}$  [8], which corresponds to an equilibrated cold-spot temperature of 40°C. When the temperature of the mercury supply was raised to 56°, the concentration of mercury above the hot spot approached  $6.95 \times 10^{14} \text{ cm}^{-3}$ , and, after equilibration, the concentration distribution presented in Fig. 2 was established. At the central plane of the discharge tube, where resonance radiation was detected, the mercury concentration was  $(n_1 - n_2)/2 = 3.44 \times 10^{14} \text{ cm}^{-3}$ , corresponding to the partial pressure of mercury equilibrated at a temperature of about 46°C, hence the absorption. The reverse process obtained near the end of the pumping cycle, approximately 52 min after the time of reversal of condensation pumps. During the following 6.6 min, the mercury number density at the discharge tube's central plane was reduced from  $3.44 \times 10^{14} \text{ cm}^{-3}$  to  $2.19 \times 10^{14} \text{ cm}^{-3}$ , corresponding to a mean cold-spot pumping speed of roughly  $8 \times 10^{13}$  particles per second.

The foregoing routine was followed for a period in excess of 300 hours for each of the three test lamps. It was found that the quartz and lead glass discharge tubes yielded diffusion time records similar to that shown in Fig. 3, indicating proper operation of the condensation pumps. The borosilicate lamp, however, produced a record with a long, slow, quasi-exponential decay, suggesting a severe deviation from the simple theory presented earlier and believed to be most likely the result of excessive sorption of mercury by the borosilicate surface combined with a temperature-dependent desorption of mercury by the surface that was absent in the other glasses.

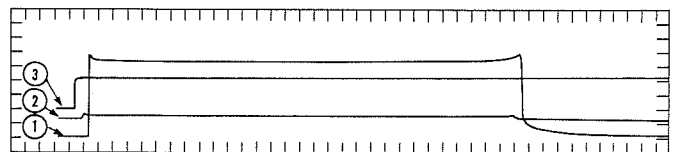


Fig. 3. Typical diffusion time record. Sweep speed is 2 minutes per division.

## V. Results and Conclusions

Measured diffusion times for mercury in lead and quartz glass discharge tubes are presented in Fig. 4. These times are proportional to the quantity of mercury present, so the slope of each line is a measure of the rate of removal of mercury by each type of glass.

The diffusion coefficients measured in the quartz, lead, and borosilicate discharge tubes were 25.12, 24.75, and 25.09  $\text{cm}^2/\text{sec}$ , respectively, with the average being 24.99  $\text{cm}^2/\text{sec}$ . This value is believed to be accurate within about 5% for mercury vapor at 75°C (the wall temperature) diffusing in argon at a pressure of 3 torr in the positive column of an arc discharge.

The unit area sorption rates for quartz and lead glass were found to be  $1.21 \times 10^{-5}$  and  $2.32 \times 10^{-5}$  cm/sec, respectively.

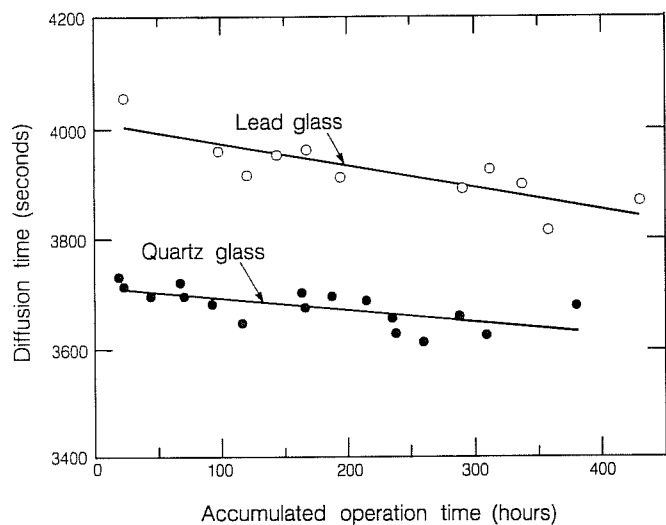


Fig. 4. Diffusion time for mercury in argon versus accumulated time of operation of lead- and quartz-glass discharge tubes.

This parameter could not be obtained for the borosilicate discharge tube.

Based on these observations, quartz glass was selected for use in the isotope blending study.

## VI. Acknowledgement

This work was supported by the Assistant Secretary for Conservation and Renewable Energy, Office of Building Energy Research and Development, Buildings Equipment Division of the U.S. Department of Energy under Contract No. DE-AC03-76SF00098.

## VII. References

- [1] R.W. Richardson and S.M. Berman, "Theory of the effects of magnetic fields and isotope enrichment on the radiant emittance of the Hg-Ar discharge," presented at the Third International Symposium on the Science and Technology of Light Sources, Toulouse, France, April 18-21 (1983), pg. 166.
- [2] R.K. Sun and S.M. Berman, "Experimental studies of enhanced emittance by isotope enrichment of a low-pressure mercury/argon discharge," presented at the Third International Symposium on the Science and Technology of Light Sources, Toulouse, France, April 18-21 (1983), pg. 166.
- [3] S. van Heusden and B.J. Mulder, "Interaction of a low pressure mercury discharge with the discharge tube wall," *Appl. Phys.* 23, p. 355 (1980).
- [4] B.J. Mulder and S. van Heusden, "Mechanism of the darkening of soda-line glass by a low pressure mercury vapour discharge," *Phys. Stat. Sol. (a)* 63, 137 (1981).
- [5] B.J. Mulder and S. van Heusden, "Mechanism of glass darkening by a low pressure mercury discharge," *J. Electrochem. Soc.* 130, p. 440 (1983).
- [6] A. Guthrie and R.K. Wakerling, *Vacuum Equipment and Techniques*, McGraw-Hill Book Co., New York (1949).
- [7] P.G. Thiene, "Convective flexure of a plasma conductor," *Phys. Fluids* 6, p. 1319 (1963).
- [8] C.W. Jerome, "Effect of bulb wall temperatures on fluorescent lamp parameters," *Illum. Engr.* 51, p. 205 (1956).